© 2016. Published by The Company of Biologists Ltd | Journal of Cell Science (2016) 129, 2156-2169 doi:10.1242/jcs.174458

RESEARCH ARTICLE

Heparin interacts with the adhesion GPCR GPR56, reduces receptor shedding, and promotes cell adhesion and motility

Nien-Yi Chiang[1], Gin-Wen Chang[1], Yi-Shu Huang[1,*], Yen-Ming Peng[2], Cheng-Chih Hsiao[1,‡], Ming-Ling Kuo[1,2,3,4] and Hsi-Hsien Lin[1,2,3,5,§]

ABSTRACT

GPR56 is an adhesion-class G-protein-coupled receptor responsible for bilateral frontoparietal polymicrogyria (BFPP), a severe disorder of cortical formation. Additionally, GPR56 is involved in biological processes as diverse as hematopoietic stem cell generation and maintenance, myoblast fusion, muscle hypertrophy, immunoregulation and tumorigenesis. Collagen III and tissue transglutaminase 2 (TG2) have been revealed as the matricellular ligands of GPR56 involved in BFPP and melanoma development, respectively. In this study, we identify heparin as a glycosaminoglycan interacting partner of GPR56. Analyses of truncated and mutant GPR56 proteins reveal two basic-residue-rich clusters, R^{26}GHREDFRFC^{35} and L^{190}KHPQKASRRP^{200}, as the major heparin-interacting motifs that overlap partially with the collagen III- and TG2-binding sites. Interestingly, the GPR56–heparin interaction is modulated by collagen III but not TG2, even though both ligands are also heparin-binding proteins. Finally, we show that the interaction with heparin reduces GPR56 receptor shedding, and enhances cell adhesion and motility. These results provide novel insights into the interaction of GPR56 with its multiple endogenous ligands and have functional implications in diseases such as BFPP and cancer.

KEY WORDS: Adhesion, GPCR, GPR56, Heparin, Glycosaminoglycan, Shedding

INTRODUCTION

G protein-coupled receptors (GPCRs) are medically important molecules, not only because they are the cause of many pathological disorders but because they are very druggable targets (Drews, 2000; Ma and Zemmel, 2002). One GPCR of great interest is the adhesion-class GPCR (adhesion GPCR) GPR56 (also known as ADGRG1) (Hamann et al., 2015; Liu et al., 1999). GPR56 was first identified in melanoma cells, where its gene expression level correlates inversely to the metastatic potential (Zendman et al., 1999). Nevertheless, it is best known as the receptor molecule solely responsible for bilateral frontoparietal polymicrogyria (BFPP), a rare human autosomal recessive disorder characterized by unique brain cortical malformations (Piao et al., 2004). More recent studies have underlined additional roles of GPR56 in male gonad development, myoblast fusion, muscle hypertrophy, oligodendrocyte development, and hematopoietic stem cell generation and maintenance (Ackerman et al., 2015; Chen et al., 2010; Giera et al., 2015; Saito et al., 2013; Solaimani Kartalaei et al., 2015; White et al., 2014; Wu et al., 2013). In the human immune system, GPR56 is expressed in a restricted manner in cytotoxic lymphocyte subsets, and its overexpression suppresses natural killer cell chemotaxis (Della Chiesa et al., 2010; Peng et al., 2011).

Unlike other GPCRs, adhesion GPCRs are characterized by an extended extracellular domain (ECD) upstream of the seven transmembrane (7TM) segment (Hamann et al., 2015; Stacey et al., 2000; Yona et al., 2008). Within the ECD, various cell-adhesion protein motifs are usually found in the N-terminal half, followed by a signature GPCR autoproteolysis-inducing (GAIN) domain that contains a consensus GPCR proteolysis site (GPS) motif (Araç et al., 2012). GPS-mediated autoproteolysis cleaves the receptor into an N-terminal ECD fragment (NTF) and a C-terminal 7TM-fragment (CTF), which then form a non-covalent complex on the cell surface. Hence, adhesion GPCRs exert their functions mostly by binding to cellular ligand(s) through the NTF and signaling through the CTF (Hamann et al., 2015; Krasnoperov et al., 2002; Lin et al., 2004).

Indeed, recent deorphanization studies of GPR56 have identified its many specific ligands. In melanoma progression, GPR56 inhibits tumor growth and metastasis by binding to and promoting the internalization and degradation of tissue transglutaminase 2 (TG2) (Xu et al., 2006; Yang et al., 2014). In brain development, the GPR56–collagen-III interaction is crucial for the integrity of the pial basement membrane and proper cerebral cortex lamination (Luo et al., 2011). In a previous report, we have described a new cellular protein ligand that interacts with the NTF of wild-type GPR56 but not with BFPP-associated point mutants (Chiang et al., 2011). In addition to the aforementioned ligands, which presumably interact with GPR56 in trans, examples of cis-acting binding partners have also been noted. As such, GPR56 has been shown to associate with the tetraspanins CD9 and CD81 (Little et al., 2004). Likewise, it was revealed that $\alpha_3\beta_1$ integrin might function synergistically with GPR56 to fine-tune cerebral cortex development (Jeong et al., 2013). Taken together, the cellular functions of GPR56 are mediated, in part, by interacting with specific protein ligands (in trans and/or in cis) on the cell surface and/or extracellular matrix (ECM).

Alternatively, adhesion GPCRs can function through receptor shedding. Indeed, ectodomain shedding has been noted for several adhesion GPCRs, including CD97, brain angiogenesis inhibitor 1 (BAI1) and GPR124 (also known as ADGRA2) (Kaur et al., 2005;

[1]Department of Microbiology and Immunology, Chang Gung University, Tao-Yuan 333, Taiwan. [2]Graduate Institute of Biomedical Sciences, College of Medicine, Chang Gung University, Tao-Yuan 333, Taiwan. [3]Chang Gung Immunology Consortium, Chang Gung Memorial Hospital and Chang Gung University, Tao-Yuan 333, Taiwan. [4]Division of Allergy, Asthma, and Rheumatology, Department of Pediatrics, Chang Gung Memorial Hospital-Linkou, Tao-Yuan 333, Taiwan. [5]Department of Anatomic Pathology, Chang Gung Memorial Hospital-Linkou, Tao-Yuan 333, Taiwan.
*Present address: The Kennedy Institute of Rheumatology, University of Oxford, Roosevelt Drive, Headington, Oxford OX3 7LF, UK. ‡Present address: Department of Experimental Immunology, Academic Medical Center, University of Amsterdam, Amsterdam, The Netherlands.

§Author for correspondence (hhlin@mail.cgu.edu.tw)

N.-Y.C., 0000-0002-9918-8079; G.-W.C., 0000-0002-6509-6897; Y.-S.H., 0000-0003-2248-2189; H.-H.L., 0000-0003-0679-5222

Received 14 May 2015; Accepted 31 March 2016

Journal of Cell Science

Journal of Cell Science (2016) 129, 2156-2169 doi:10.1242/jcs.174458

Vallon and Essler, 2006; Wang et al., 2005). Shedding is likely to generate distinct soluble receptor fragments that have different cellular functions from the membrane-bound proteins. Previously, we and others have detected the presence of soluble GPR56 (sGPR56; the NTF that has been shed from the membrane) in transfected cells, suggesting constitutive GPR56 shedding (Chiang et al., 2011; Jin et al., 2007; Yang et al., 2015). More intriguingly, expression of a truncated GPR56 receptor that lacked the NTF was shown to signal constitutively (Paavola et al., 2011). Similarly, deletion of the TG2-binding Ser–Thr–Pro-rich (STP) segment within the GPR56 NTF also enhances melanoma tumor growth and angiogenesis significantly (Yang et al., 2011). A more recent study has shown that GPR56 is activated by a cryptic tethered agonist peptide that is located at the most N-terminal end of the CTF and exposed following the dissociation of the NTF (Stoveken et al., 2015). Finally, binding of collagen III to GPR56 promotes the release of the GPR56 NTF from the CTF, which then relocates to the lipid raft microdomain for RhoA activation (Luo et al., 2014; Schoneberg et al., 2015). Taken together, the GPR56 NTF might act as a repressor of the constitutively active CTF, whose signaling activity is turned on by the exposure of a tethered agonist upon removal of the NTF (Liebscher et al., 2015; Stoveken et al., 2015). Thus, the signaling activity of GPR56 might be modulated through the interaction of its cellular binding partners with the NTF, or alternatively by shedding of the NTF.

In addition to interacting with protein ligands, adhesion GPCRs have also been shown to interact with non-protein molecules, such as polysaccharides, and phospholipids and glycolipids. These include phosphatidylserine (PS) and lipopolysaccharide (LPS) for BAI1, as well as glycosaminoglycans (GAGs) for CD97, EMR2 (also known as ADGRE2) and GPR124 (Das et al., 2011; Hochreiter-Hufford et al., 2013; Stacey et al., 2003; Vallon and Essler, 2006; Wang et al., 2005). Heparin and the closely related heparan sulfate, and chondroitin sulfate (also known as dermatan sulfate) are the most abundant GAGs attached to proteoglycans. They are defined by the composition of their amino sugars and the different degrees of modification on the sugars, such as epimerization and sulfation, which create structural complexities directly linked to functional variability (Bernfield et al., 1999; Carlsson et al., 2008; Esko et al., 2009). Herein, we report the identification of heparin as a GAG interacting partner of GPR56 and characterize the functional consequence of the GPR56–heparin interaction.

RESULTS

Specific interaction of the GPR56 NTF with heparin

In addition to protein ligands, certain adhesion GPCRs such as CD97, EMR2 and GPR124 also interact with GAGs, the polysaccharide components of proteoglycans (Stacey et al., 2003; Vallon and Essler, 2006; Wang et al., 2005). In an attempt to define the new cellular ligand of GPR56 described in our previous report (Chiang et al., 2011), we examined and concluded that collagen III is unlikely to be the putative cellular ligand (Fig. S1). We hence decided to test the possibility of a GPR56–GAG interaction. We employed a modified enzyme-linked immunosorbent assay (ELISA) using plate-bound GAGs and detected strong binding of a GPR56 and mouse fragment crystallizable fusion protein (GPR56–mFc) to heparin, as well as a much weaker interaction with heparan sulfate and chondroitin sulfate-B (Fig. 1A). In contrast, binding of GPR56–mFc to chondroitin sulfate-A, chondroitin sulfate-C and hyaluronic acid was negligible. As expected, the control mFc protein showed no binding to any of the GAGs tested. Importantly, the GPR56–heparin interaction was inhibited in a dose-dependent manner by exogenously added heparin, thus confirming the specificity of the reaction (Fig. 1A,B). Likewise, an alternative heparin–agarose pulldown assay showed that only GPR56–mFc, but not mFc or EMR2–mFc protein, was captured and precipitated by the heparin–agarose beads (Fig. 1C). As EMR2 is a similar highly glycosylated adhesion GPCR with a unique binding affinity to chondroitin sulfate, these results further verify that the GPR56–heparin interaction is specific and not just the result of the 'sticky' nature of adhesion GPCRs. When tested at the same molar concentrations, GPR56 showed stronger binding than IL-8 – a well-known heparin-binding protein – to heparin, suggesting a potential higher heparin-binding reactivity of GPR56 (Fig. 1D). These results clearly indicate that heparin is a specific GAG binding partner of GPR56.

Characterization of GPR56–heparin interaction

To characterize the GPR56–heparin interaction further, a GPR56–heparin binding assay was performed in the presence or absence of EDTA or EGTA with or without extra divalent cations (Ca^{2+} or Mg^{2+}). As shown in Fig. 2A, the GPR56–heparin interaction was impaired by the addition of EDTA or EGTA. On the contrary, the interaction was greatly enhanced by the addition of Ca^{2+} or Mg^{2+}. Likewise, GPR56–mFc protein that had been pulled down by heparin–agarose beads was efficiently uncoupled from the agarose beads by EDTA- or EGTA-containing buffer (Fig. 2B) (data not shown). We thus conclude that the GPR56–heparin interaction is dependent on divalent cations.

As GPR56 deficiency is a direct cause of BFPP, we next examined the heparin-binding characteristics of selected BFPP-associated GPR56 point mutants (Piao et al., 2004). In addition, the heparin-binding ability of human versus mouse GPR56 proteins was also compared because the two proteins have been shown previously to have different TG2-binding properties (Chiang et al., 2011). Interestingly, both solid-phase heparin-binding and heparin–agarose pulldown assays showed that the relevant BFPP mutants (GPR56-R38W, GPR56-Y88C and GPR56-C91S) displayed a much stronger heparin-binding ability than the wild-type protein (Fig. 2C,D). This result indicates that heparin (or heparan sulfate) is not the new cellular ligand of GPR56 that our studies have previously alluded to, and to which the BFPP mutants are unable to bind (Chiang et al., 2011). By contrast, mouse GPR56 showed a specific but weaker interaction with heparin in comparison to human GPR56 (Fig. 2C,E). This is true even when the binding was tested in an alternative ELISA-based assay whereby biotinylated heparin was incubated with plate-bound GPR56–mFc fusion proteins (Fig. 2F). We conclude that the heparin-binding activity is conserved in both human and mouse GPR56 proteins. In addition, the heparin-binding activity of GPR56 can be greatly modulated by single amino acid changes, as attested by the stronger heparin-binding BFPP-causing point mutants.

Mapping the heparin-binding sites in GPR56

The specificity and affinity of protein–GAG interactions vary widely, and generally involve the electrostatic interaction of basic amino acids with the negatively charged GAGs (Hileman et al., 1998). Thus, the heparin-binding sites usually contain clusters of basic amino acids in a linear sequence and/or in specific conformational ensembles. To date, two well-known linear heparin-binding motifs, namely XBBXB and XBBBXXBX (B represents a basic amino acid, and X is any neutral or hydrophobic residue), are identified (Cardin and Weintraub, 1989). A survey of the human GPR56 NTF found a reverse

Journal of Cell Science (2016) 129, 2156-2169 doi:10.1242/jcs.174458

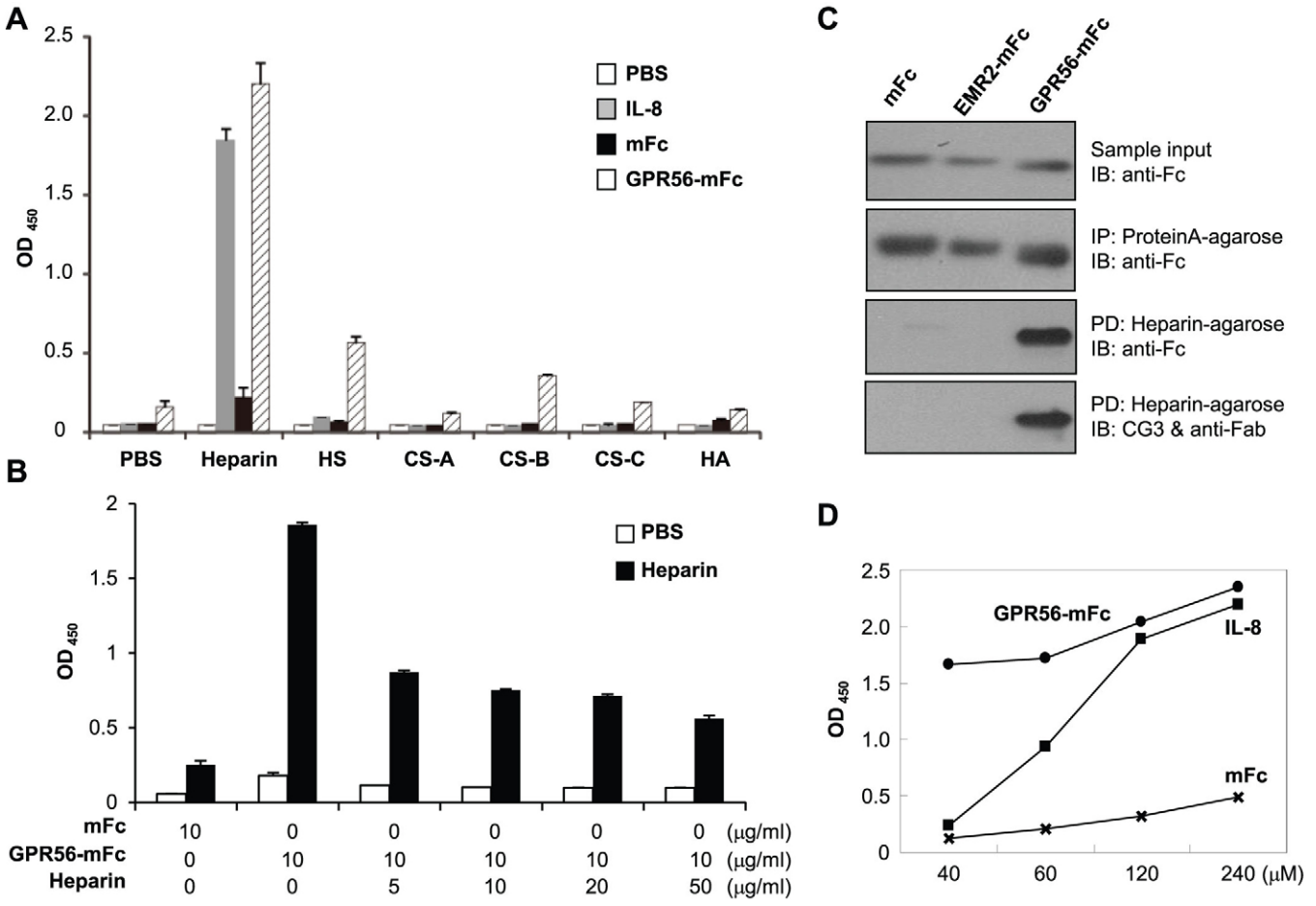

Fig. 1. Heparin is a specific GAG ligand for GPR56. (A) A GPR56–heparin interaction was detected using a modified ELISA-based analysis using the BD™ heparin-binding plate. Plates are pre-coated with different types of GAG molecules (25 µg/ml), as indicated (HS, heparin sulfate; CS, chondroitin sulfate; HA, hyaluronic acid). Plates were incubated with various protein probes, as indicated, and the binding was detected as described in Materials and Methods. IL-8 was used as a heparin-binding protein control. (B) GPR56–mFc was incubated with the heparin-coated plates as described, either alone or in the presence of exogenous heparin as indicated. Plates containing PBS only were used as a negative control. (C) An alternative heparin–agarose pulldown assay to confirm the specific GPR56–heparin interaction. Conditioned media containing mFc-fusion proteins were either unmanipulated (input control, top panel), precipitated with protein-A–agarose (positive control, the second panel) or with heparin–agarose beads (the third and bottom panels) followed by western blotting using anti-mFc or the anti-GPR56 CG3 mAb. (D) Demonstration of the dose-dependent interaction of GPR56 with heparin. Different concentrations of protein probes were used in the modified ELISA assay as indicated. mFc and IL-8 were used as a negative control and heparin-binding protein control, respectively. All data are means±s.e.m. of three independent experiments performed in triplicate.

XBBXB consensus sequence (**R**^{26}G**HR**EDF**R**^{33}, basic residues in bold), and several XBBX clusters (Fig. 3A,B) (data not shown).

To identify and verify the putative heparin-binding region(s), a series of truncated GPR56–mFc fusion proteins were engineered, and their relative heparin-binding activity was determined (Fig. 3A; Fig. S2). We found that the majority of the C-terminal truncation proteins still retained the heparin-binding activity, suggesting the presence of a dominant heparin-binding sequence at the most N-terminal region. Indeed, although heparin-binding was not observed in a mutant comprising the first 25 amino acids of [GPR56(1–25)–mFc], a weak binding signal was readily detected in GPR56(1–30)–mFc. Most interestingly, a much stronger heparin-binding signal was noted in GPR56(1–35)–mFc protein and other larger C-terminally truncated proteins. As the first 25 amino acid residues constitute the signal peptide of GPR56, the GPR56(1–25)–mFc protein was essentially the same as the negative control mFc-only protein. These results support the notion that the region between residues 26 and 35 of GPR56 constitutes a heparin-binding site (Fig. 3B,C).

To verify the role of the R^{26}GHREDFRFC^{35} motif in heparin-binding, two GPR56(1–35)–mFc mutants, one with residue Arg33 mutated to Ala [GPR56(1–35/R33A)] point mutation and the other with three mutations of His28, Arg29 and Arg33 to Ala, were generated [GPR56(1–35/H28/R29/R33A)] (Fig. 3B; Fig. S3A–C). Interestingly, although the R33A mutation slightly reduced the heparin-binding activity of GPR56(1–35)–mFc, the GPR56(1–35/H28/R29/R33A) triple mutant almost completely abrogated heparin binding (Fig. 3C). These results confirmed that the R^{26}GHREDFR^{33} motif is indeed the N-terminal heparin-binding domain of GPR56 with a significant contribution from His28, Arg29 and Arg33 residues.

Apart from the R^{26}GHREDFR^{33} motif, additional heparin-binding regions were also present as positive heparin-binding activities were noted to similar extents in various N-terminally truncated GPR56–mFc fusion proteins (Figs S2 and S3D,E). Several potential heparin-binding XBBX clusters were noted in the C-terminal half of the GPR56 NTF and, hence, were investigated further. Among them, the L^{190}**KH**PQ**K**AS**RR**P^{200} region with two

Journal of Cell Science (2016) 129, 2156-2169 doi:10.1242/jcs.174458

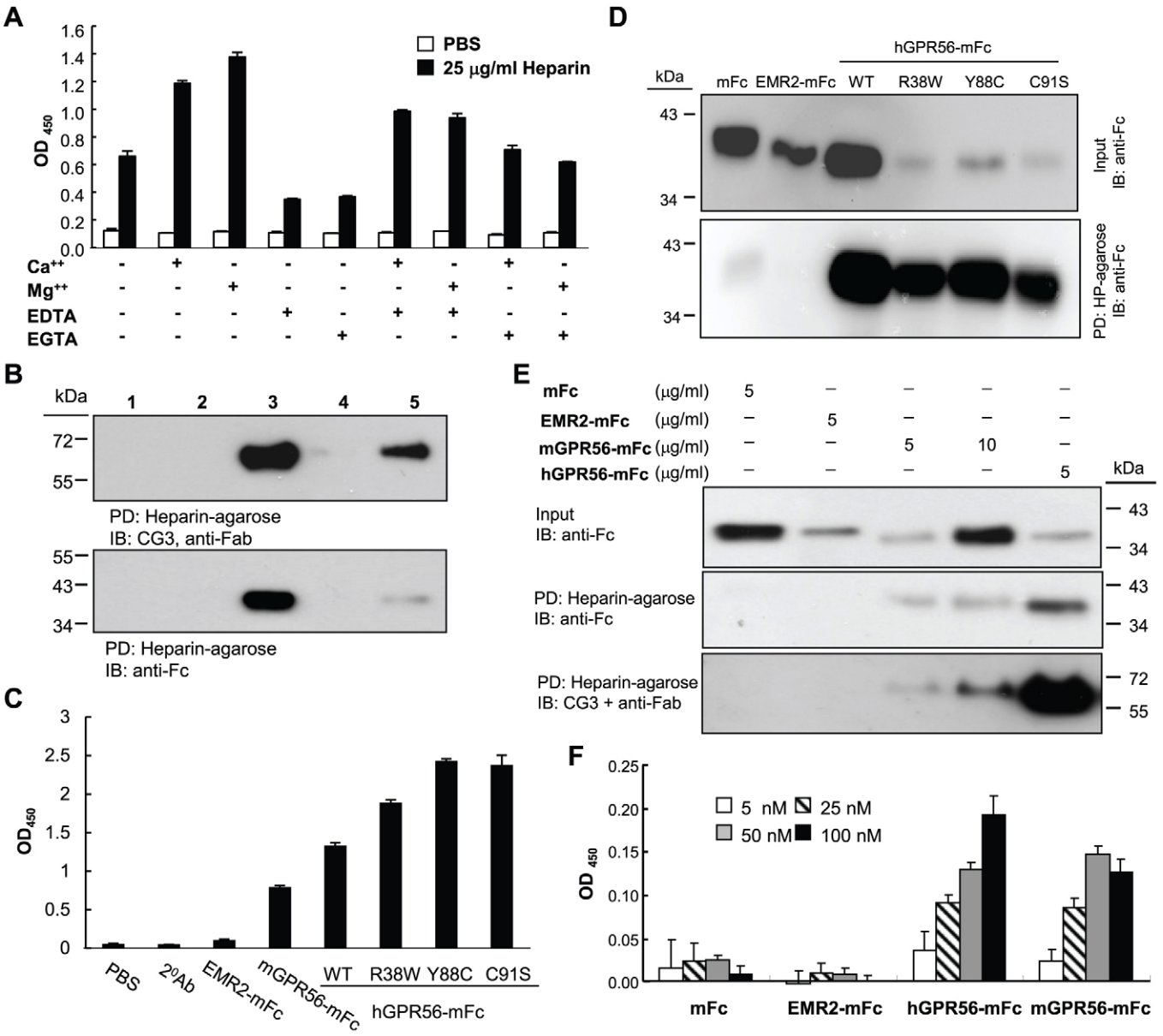

Fig. 2. Biochemical characterization of GPR56–heparin interaction. (A) The modified ELISA heparin-binding assay was carried out in the presence of EDTA or EGTA (10 mM) with or without exogenous divalent cations (Ca^{2+} or Mg^{2+}, 10 mM). (B) Western blot analysis of the heparin pulldown (PD) assay performed using purified mFc (lane 1), EMR2–mFc (lane 2) and GPR56–mFc proteins (lanes 3–5). Precipitated GPR56–mFc was analyzed directly (lane 3) or incubated with PBS–EDTA (10 mM) buffer to separate pellet (lane 4) and eluate (lane 5). Blots were probed with specific antibodies (immunoblot, IB) as indicated. (C–F) Comparison of the heparin-binding activities of the human and mouse GPR56 proteins (hGPR56 and mGPR56, respectively), and indicated BFPP-associated point mutants. Heparin binding was detected using the modified ELISA analysis (C), the heparin (HP)–agarose pulldown assay (D,E) and an alternative ELISA-based assay in which biotinylated heparin (10 μg/ml) was used to interact with the plate-bound mFc-fusion proteins as indicated (F). All data are means±s.e.m. of three independent experiments performed in triplicate. 2^0Ab, secondary antibody only; WT, wild type.

XBBX sequences was of interest because mutation of the basic residues to Ala greatly reduced the heparin-binding activity of the GPR56(1–340)–mFc protein, which contains most of the NTF, except the GPS motif (Fig. 3A,B,D; Figs S2, S3D,E). Combined mutation of the basic residues in the R^{26}GHREDFR^{33} and the L^{190}KHPQKASRRP^{200} regions showed a synergistically diminished heparin-binding activity (Fig. 3B,D; Fig. S3D,E). Interestingly, similar abilities to bind to collagen III were detected in the wild-type GPR56(1–340)–mFc protein and the various mutant probes tested, indicating that these basic residues are not involved in the GPR56–collagen-III interaction (Fig. 3D). Taken together, we conclude the R^{26}GHREDFR^{33} and L^{190}KHPQKASRRP^{200} clusters constitute the two major heparin-binding regions of GPR56.

Distinct effects of the ternary GPR56–heparin–protein-ligand interaction

As an important component of proteoglycans and ECM molecules, GAGs interact with a plethora of soluble cell surface and matrix proteins to modulate their functions either positively or negatively (Funderburgh, 2000; Rabenstein, 2002; Trowbridge and Gallo, 2002). In fact, the two known matricellular ligands of GPR56, collagen III and TG2, have both been reported to interact with heparin (Lortat-Jacob et al., 2012; San Antonio et al., 1994). More

Journal of Cell Science (2016) 129, 2156-2169 doi:10.1242/jcs.174458

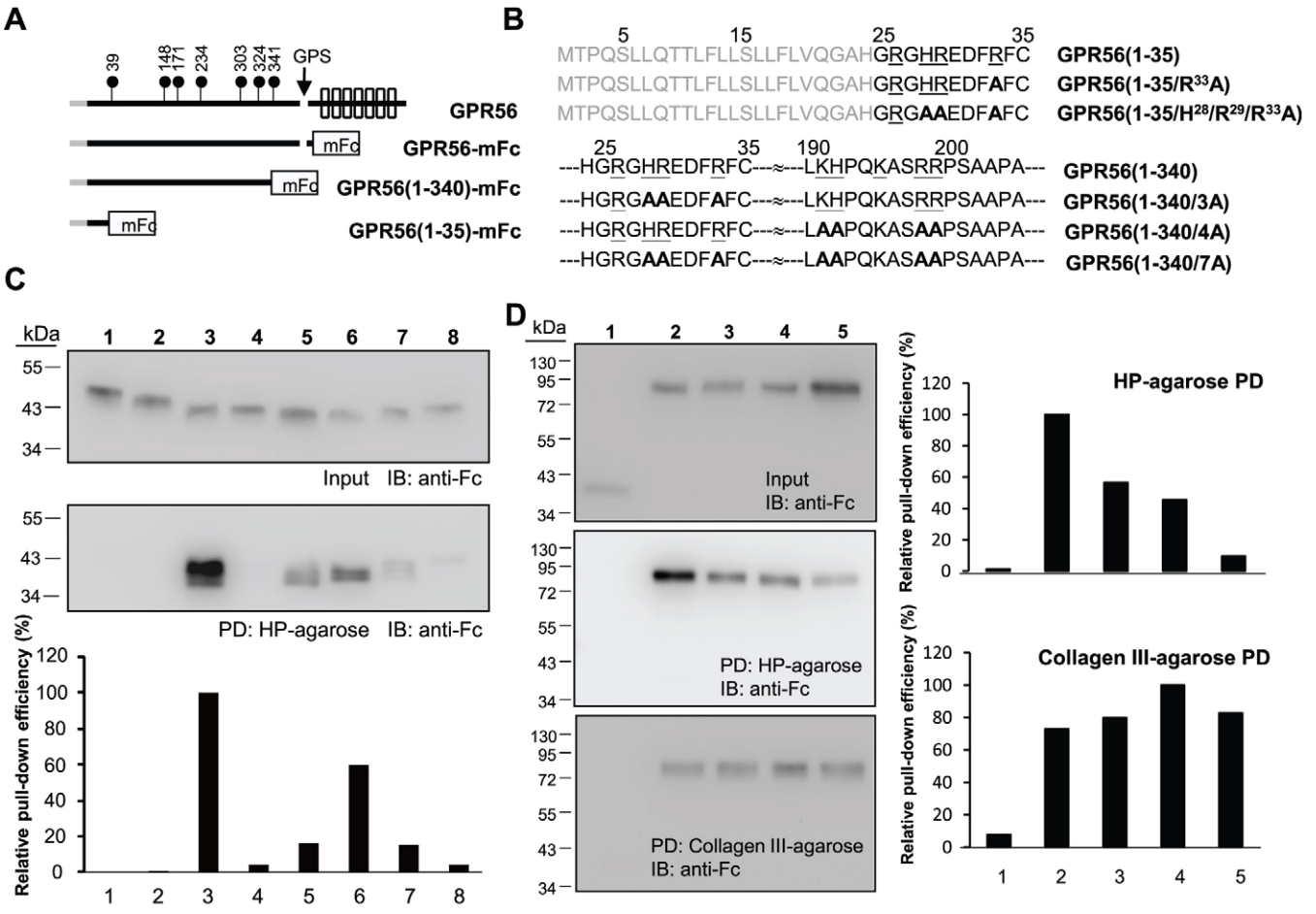

Fig. 3. Mapping of the potential heparin-binding sites in GPR56. (A) Schematic diagrams showing some of the truncated GPR56–mFc fusion proteins used in the analysis. The numbers along the top denote the amino acid residues that are N-linked glycosylation sites. The signal peptide and 7TM region are represented by a gray line and seven rectangles, respectively. (B) Sequence information of the point mutations introduced into the truncated GPR56–mFc probes used to identify the heparin-binding sites. Gray residues, the signal peptide; underlined residues, the hydrophobic residues; bold residues, site-directed mutants. Number along the top indicate amino acid positions. (C) Western blotting (IB) analysis of the *in vitro* heparin (HP)–agarose pulldown (PD) assay. The input control (upper panel) and heparin–agarose pull down (middle panel) were subjected to SDS-PAGE and detected with the anti-Fc antibody. The graph shows the relative pulldown efficiencies by comparing the band intensity of the input and the pulldown blots with the result of GPR56–mFc (lane 3) set as 100% (lower panel). The samples analyzed include: mFc alone (lane 1), EMR2–mFc (lane 2), GPR56–mFc (lane 3), GPR56(1–25)–mFc (lane 4), GPR56(1–30)–mFc (lane 5), GPR56(1–35)–mFc (lane 6), GPR56 (1–35/R33A)–mFc (lane 7), and GPR56(1–35/H28/R29/R33A)–mFc (lane 8). Data shown are one representative of three independent experiments with similar results. (D) Western blotting analysis and quantitative comparison of the *in vitro* heparin–agarose and collagen-III–agarose pulldown assays of the EMR2–mFc (lane 1), GPR56(1–340)–mFc (lane 2), GPR56(1–340/3A)–mFc (lane 3), GPR56(1–340/4A)-mFc (lane 4) and GPR56(1–340/7A)–mFc (lane 5) proteins. The intensity of the protein band was quantified using Gel-Pro Analyzer 3.1. Data shown are one representative of three independent experiments with similar results.

interestingly, a functional collagen-III-binding region has been identified within the region between residues 27 and 160 of GPR56, which overlaps with the heparin-binding $R^{26}GHREDFR^{33}$ motif (Luo et al., 2012). By contrast, the TG2-binding STP segment has been located in the region between positions 108 and 177 (Yang et al., 2011), which is distinct from but proximal to another heparin-binding $L^{190}KHPQKASRRP^{200}$ region. The partial overlapping and close proximity of the heparin-binding motifs to the collagen III- and TG2-binding regions strongly suggests that heparin is likely to enhance or hinder the interaction of GPR56 and its protein ligands.

Hence, we examined the potential outcome of the ternary GPR56–heparin–protein-ligand interaction. As shown in Fig. 4A, pre-incubation of collagen III with heparin reduced the GPR56–heparin interaction significantly, but no such inhibitory effect was observed when collagen III was added simultaneously with GPR56–mFc. Similar results were obtained using agarose pulldown assays with both the heparin–agarose and collagen-III–agarose beads (Fig. S3F, lane 4). Interestingly, pre-incubation of GPR56 and heparin greatly enhanced the amount of GPR56 pulled down by collagen-III–agarose, but pre-incubation of GPR56 and collagen III did not further increase the GPR56 pulldown efficiency of heparin–agarose (Fig. S3F, lane 3). Hence, it seems that the strength and outcome of the ternary GPR56–heparin–collagen-III interaction might depend on the binding sequence among these three molecules. By contrast, no apparent difference was found in the GPR56–TG2 far-western binding assay when either probed sequentially with heparin followed by GPR56–mFc or by heparin and GPR56–mFc together at the same time (Fig. 4B).

Surprisingly, we found that the interaction of GPR56 with the new cellular ligand that had been previously described by us could be modulated bilaterally with GAGs (Fig. 4C,D). As such, it was noted that heparin inhibited, whereas heparan sulfate and chondroitin sulfate-B enhanced, GPR56 binding to the cellular ligand if GAGs and the GPR56–mFc probe were added simultaneously (Fig. 4C). If cells were allowed to incubate with GAGs first, the GPR56–cellular-ligand interaction was enhanced

Journal of Cell Science (2016) 129, 2156-2169 doi:10.1242/jcs.174458

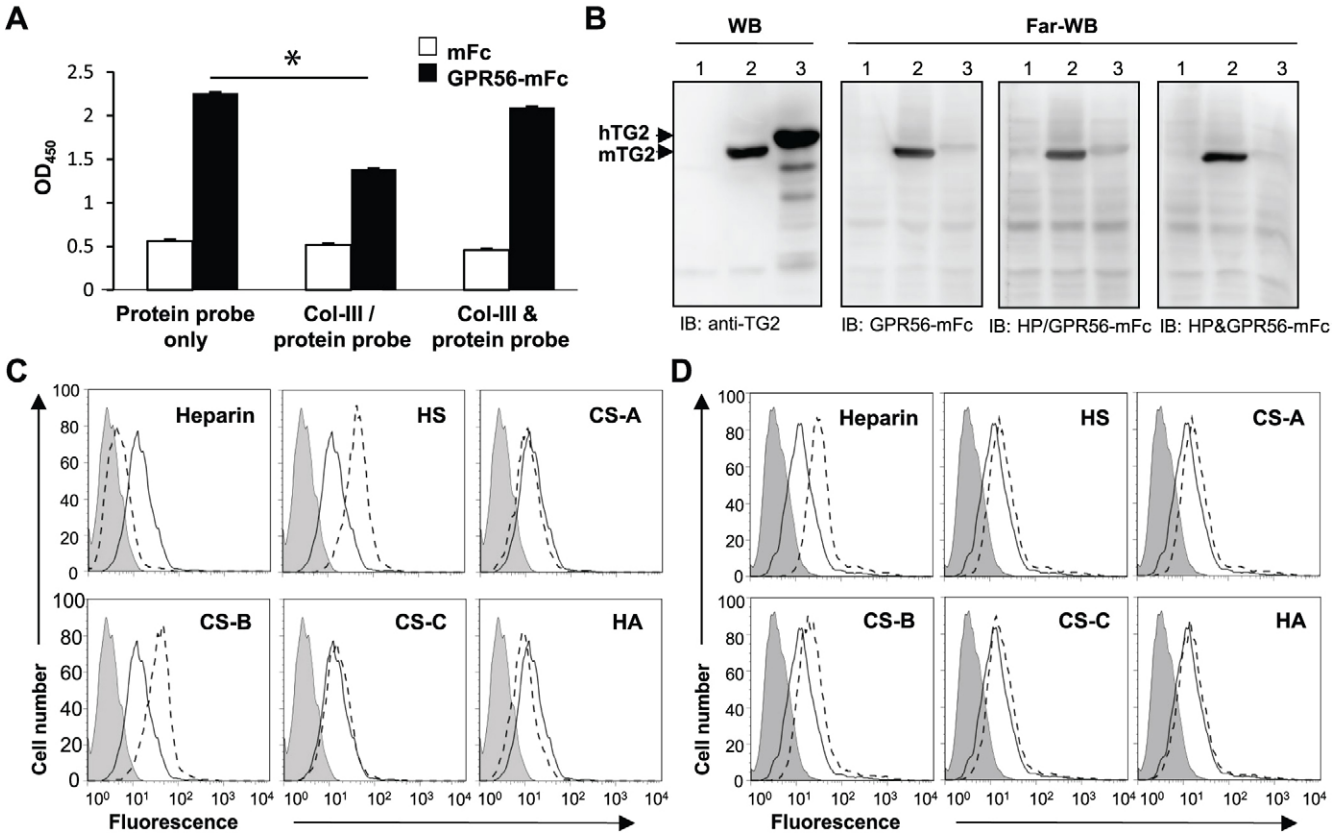

Fig. 4. Distinct effects of the trimeric GPR56–heparin–protein ligand interaction. (A) Modulation of GPR56–heparin binding by collagen III. Plate-bound heparin was incubated with protein probes (mFc or GPR56–mFc, 10 µg/ml each) alone, collagen III first, followed by protein probes (col-III/protein probe), or protein probes and collagen III together (col-III & protein probe). Data are means±s.e.m. of three independent experiments performed in triplicate. (B) The GPR56–TG2 interaction was evaluated by far-western blotting, as described in the Materials and Methods. Total cell lysates of HEK-293T cells that had been transfected without (lane 1) or with mouse TG2 (lane 2, mTG2) or human TG2 (lane 3, hTG2) expression constructs were analyzed by western blotting using an anti-TG2 mAb (left panel). The same blots were incubated with the GPR56–mFc probe only, first with heparin (HP) followed by GPR56–mFc probe (HP/GPR56–mFc), or heparin and GPR56–mFc probe together (HP & GPR56–mFc). (C,D) Differential modulation of GPR56 binding to the putative cell surface ligand by GAGs. HT1080 cells were incubated with the GPR56–mFc probes in the absence or presence of various GAGs (20 µg/ml) as indicated. The extent of GPR56-binding was determined with FACS analysis. Cells were either probed with GPR56–mFc and GAGs together (C) or pre-incubated with GAGs, followed by GPR56–mFc (D). The gray background represents the cell-only control, and the black line and dashed line represents GPR56–mFc alone and GPR56–mFc plus GAGs, respectively. CS, chondroitin sulfate; HA, hyaluronic acid; HS, heparan sulfate.

greatly by heparin but only slightly by heparan sulfate and chondroitin sulfate-B (Fig. 4D). Interestingly, other GAGs, such as chondroitin sulfate-A, chondroitin sulfate-C and hyaluronic acid, had no effects on the GPR56–cellular-ligand binding in both conditions. These results imply that GPR56 mediates the interaction with heparin and the novel cellular ligand through similar or overlapping binding region(s). Furthermore, as with collagen III and TG2, the new cellular ligand itself might be able to bind to specific GAGs as well. Taken together, these data suggest that heparin is able to modulate the interaction of GPR56 with its protein ligands selectively and vice versa.

The heparin–GPR56 interaction reduces GPR56 receptor shedding and promotes cell adhesion and motility

GPR56 has been shown previously to regulate cell migration, but the precise mechanism is not fully understood. A well-established role of heparin (or heparan sulfate) is to interact with various growth factors, chemokines and ECM proteins (Rabenstein, 2002; Salmivirta et al., 1996). This action generally leads to phenotypic changes in cellular adhesion and motility. We therefore tested the effect of heparin on GPR56-medited cell adhesion and migration. For the cell adhesion assay, GPR56^{dim} A375 melanoma cells (expressing low levels of surface GPR56) were engineered to overexpress GPR56 and incubated with various forms of plate-bound heparin. As shown in Fig. 5, stronger cell adhesion was detected in GPR56-expressing A375 (A375-GPR56) cells than in the control A375-Neo cells. Interestingly, no significant differences were found in the adhesion of A375-GPR56 cells to low- or high-molecular-mass heparins, or to unfractionated heparins (Fig. 5). For the cell migration assay, highly mobile HT1080 cells stably expressing GPR56 (HT1080-GPR56) were subjected to the Boyden chamber-based chemotaxis assay using fetal calf serum (FCS) as a chemoattractant. HT1080-Neo cells were included as a control. The extent of cell migration was compared without or with heparin added in the upper or lower chamber. In the absence of heparin, both stable cell lines displayed comparable migration abilities toward a range of FCS concentrations (2% and 10%), indicating similar basal chemotactic motilities (Fig. 6A). When heparin was placed in the upper chamber, HT1080-GPR56 cells showed a ~twofold increase over HT1080-Neo cells in chemotactic migration toward 2% and 10% FCS (Fig. 6A). In contrast, no significant difference in cell migration was observed in both cell lines if heparin was placed in the lower chamber (Fig. 6B). Likewise, a similar enhancing effect of heparin on cell invasion was

Journal of Cell Science (2016) 129, 2156-2169 doi:10.1242/jcs.174458

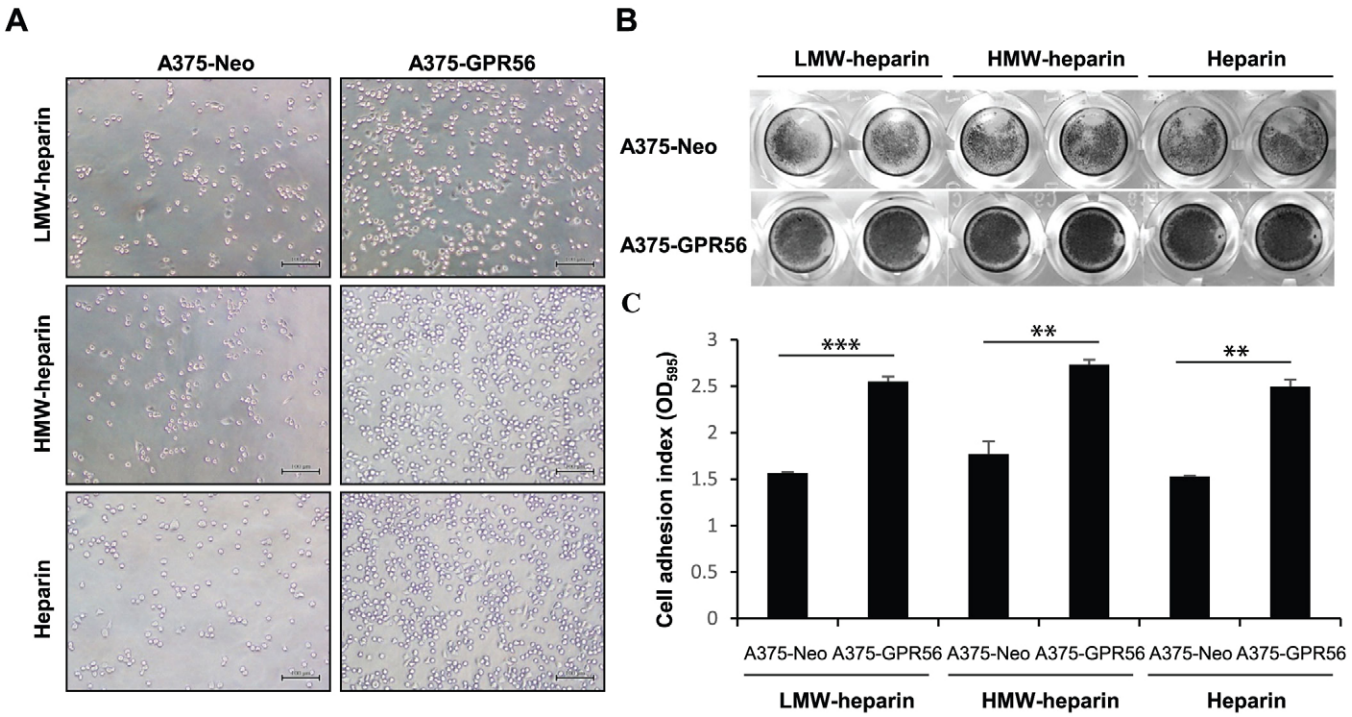

Fig. 5. Analysis of the effect of heparin-GPR56 interaction on cell adhesion. (A–C) A375 cells stably expressing the indicated constructs (A375-Neo and A375-GPR56) were incubated in wells that had been pre-coated with different types of heparins, including low-molecular-mass (LMW) heparin, high-molecular-mass (HMW) heparin, and unfractionated heparin (20 µg/ml) for 30 min. Following extensive washes, adherent cells were observed under a microscope (A), or stained with 1% methylene blue (B). Cells were lysed, and the dye was dissolved in ethanol for the measurement of cell adhesion efficiency at OD_{595} (C). All data are means±s.e.m. of three independent experiments performed in triplicate. *P<0.05, **P<0.01, ***P<0.001, A375-GPR56 cells vs A375-Neo control cells (Student's t-test). Scale bars: 100 µm.

observed only when heparin was placed in the upper chamber (Fig. 6C). These results suggest that heparin can somehow promote cell chemokinesis (random cell migration) but not chemotaxis (directional cell migration) through binding to GPR56.

Previous studies by Luo et al. have shown that the GPR56–collagen-III interaction inhibits the migration of neural progenitor cells (NPCs) (Luo et al., 2011). It has been further demonstrated recently that binding of collagen III to GPR56 enhances the dissociation (shedding) of the GPR56 NTF (sGPR56) from its CTF, which then relocates to the lipid raft microdomains and induces RhoA activation (Luo et al., 2014). In melanoma cells, GPR56 has been shown to inhibit VEGF production through a protein kinase Cα (PKCα)-mediated signaling pathway (Yang et al., 2011). Furthermore, TG2 binding to GPR56 promotes receptor-mediated internalization and subsequent degradation of TG2, and secreted GPR56 NTF competes and blocks the binding and internalization of TG2 by GPR56 (Yang et al., 2014). To investigate the potential mechanism(s) involved in the heparin-enhanced cell adhesion and motility, the effect of heparin on the cellular distribution of GPR56 receptor subunits, activation of signaling molecules and GPR56 receptor shedding were examined. Unlike collagen III, the interaction of heparin with GPR56 did not promote the relocation of the CTF to the lipid raft microdomains (Fig. 7A), nor the activation of RhoA (Fig. 7B). Likewise, no significant PKCα activation was identified in heparin-treated GPR56-expressing cells (Fig. 7C). Interestingly, however, an inhibitory effect on collagen-III-induced RhoA activation was observed in GPR56-expressing cells that had been either pre-incubated with heparin or incubated simultaneously with heparin and collagen III (Fig. 7D; Fig. S3G). This inhibitory effect was not found when heparin was added after GPR56-expressing cells had been treated with collagen III (Fig. 7D; Fig. S3G). More interestingly, sGPR56 that had been derived from transiently transfected HEK-293T cells was reduced significantly and in a dose-dependent manner in the presence of heparin (Fig. 7E). Moreover, C32 melanoma cells that expressed endogenous GPR56 also shed less sGPR56 when cultured in the presence of heparin (Fig. 7F). Finally, similar data were obtained in stable GPR56-expressing HT1080 cells (Fig. 7G). These results indicate that heparin binding to GPR56 reduces GPR56 receptor shedding without affecting the membrane distribution patterns of the GPR56 NTF and CTF. Moreover, here, no evidence of GPR56-induced signaling by heparin has been found, rather it seems that heparin acts as an inhibitory modulator preventing collagen-III-induced GPR56 activation by hindering the collagen-III–GPR56 interaction. In this sense, heparin could be considered an antagonist of the GPR56 receptor. It remains to be demonstrated whether the heparin–GPR56 interaction induces intracellular signaling.

DISCUSSION

In addition to the well-known protein ligands collagen III and TG2, we have identified heparin (and heparan sulfate) as the GAG interacting partner of GPR56 (Figs 1 and 2). The GPR56–heparin interaction is dependent on divalent cations, is conserved in human and mouse receptors, and can be specifically blocked by exogenous heparin. Through the use of truncated and mutated GPR56 protein probes, the major heparin-binding regions were mapped to two distinct basic-residue-rich motifs in the GPR56 NTF, which overlap partially with the collagen-III- and TG2-binding sites (Fig. 3). Our finding expands the repertoire of endogenous binding partners of GPR56 and suggests that the

Journal of Cell Science (2016) 129, 2156-2169 doi:10.1242/jcs.174458

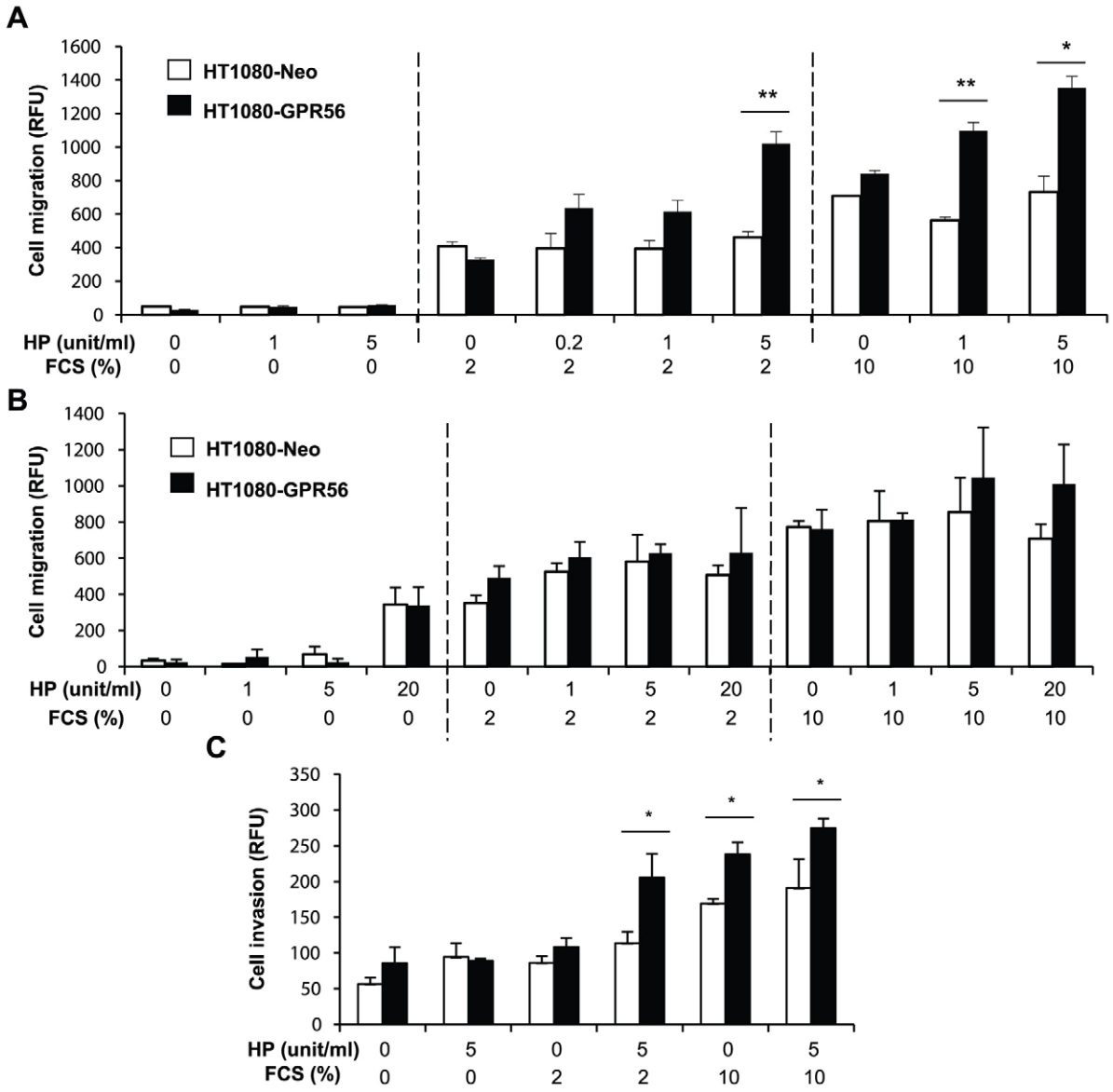

Fig. 6. Analysis of the effects of the heparin–GPR56 interaction on the migration and invasion of HT1080 cells. (A,B) HT1080 cells (1×10^5 cells) were incubated for 6 h in the Boyden chamber. Cells that had migrated were stained and measured with excitation at 480 nm and emission at 520 nm. Heparin was added to the upper chamber (A) or the lower chamber (B). When heparin (HP) was added in the upper chamber, twice as many cells stably expressing GPR56 migrated into the lower chamber as compared with HT1080-Neo control cells. (C) Heparin enhances the invasion activity of HT1080-GPR56 stable cells *in vitro*. HT1080 cell invasion was assayed using the various concentrations of FCS as chemoattractant. Invasion was assayed using the Millipore Cell invasion assay. All data are means±s.e.m. of three independent experiments performed in triplicate. **P*<0.05, ***P*<0.01, HT1080-GPR56 vs HT1080-Neo control (Student's *t*-test).

ubiquitous heparin (heparan sulfate) GAG might regulate GPR56 receptor function.

Heparin and heparan sulfate are closely related GAGs with variably sulfated repeating disaccharide units. The major disaccharide unit of heparin comprises 2-O-sulfated iduronic acid (IdoA2S) and 6-O-sulfated N-sulfated glucosamine (GlcNS6S), whereas the most common disaccharide repeat of heparan sulfate is a glucuronic acid moiety (GlcA) linked to N-acetylglucosamine (GlcNAc). Further complexity and variability arises when the length, arrangement and degrees of modification of the disaccharide units are considered (Bernfield et al., 1999; Esko et al., 2009). Although heparin is naturally produced and stored in the granules of mast cells and heparan sulfate is ubiquitously present on proteoglycans, it is possible to have 'heparin-like' and 'heparan-sulfate-like' GAGs on the same proteoglycan (Bernfield et al., 1999; Carlsson et al., 2008). The heparin-like and heparan-sulfate-like GAGs are known to have different affinities for specific proteins, hence variable functional outcomes. Our finding of the stronger GPR56 binding to heparin over that to heparan sulfate might suggest a preferential affinity of the GPR56 protein to certain modified disaccharides of heparin-like GAGs. Most interestingly, GPR56 is shown to bind equally well to heparin species of both low- and high-molecular masses, confirming its unique affinity to the heparin-like GAG structure (Fig. 5). It is worth noting that GPR56 protein does not bind to other GAGs, such as chondroitin sulfate and hyaluronic acid, indicating again that the heparin-binding ability of GPR56 is specific and not due to the 'sticky' nature of adhesion GPCRs (Fig. 1). This is especially true when we compare GPR56 and EMR2, another well-known chondroitin-sulfate-binding adhesion GPCR (Fig. 1C).

Journal of Cell Science (2016) 129, 2156-2169 doi:10.1242/jcs.174458

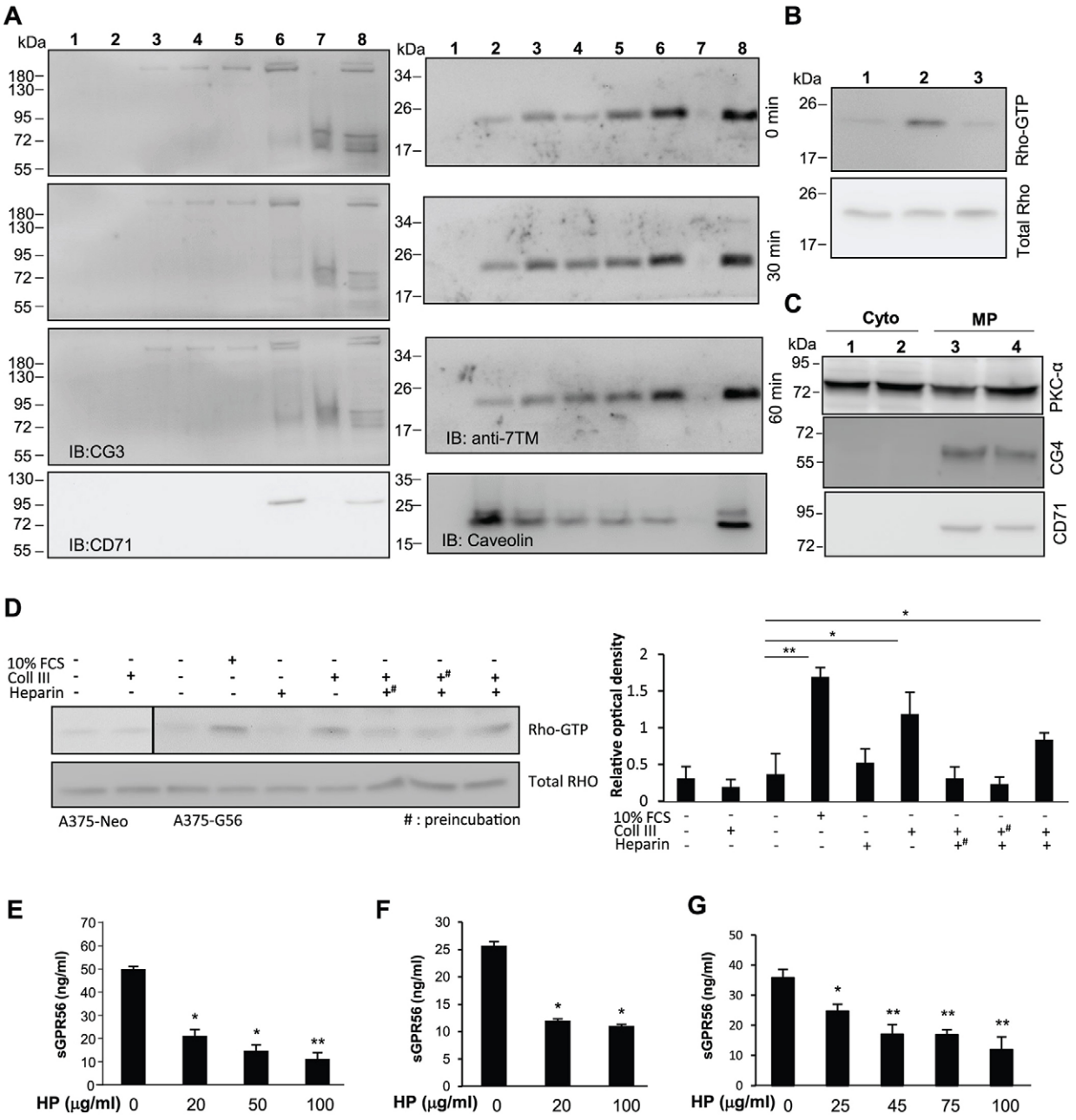

Fig. 7. Heparin reduces constitutive GPR56 shedding, with no effect on the lipid raft distribution pattern of the GPR56 CTF or on activation of RhoA and PKCα. (A) HT1080 cells stably expressing GPR56 were stimulated with heparin (20 µg/ml) for the indicated period of time (0, 30, and 60 min) and then subjected to lipid raft separation, as described in the Materials and Methods. Western blot (IB) analysis of equal volumes of seven distinct ultracentrifuged fractions (lanes 1–7) and total cell lysate (lane 8) were probed to detect the GPR56 NTF and CTF with CG3 mAb (three top left panels) and anti-7TM antibodies (three top right panels), respectively. The NTF is detected at 60–70 kDa owing to glycosylation, and protein aggregates are observed at the top of the gel. Caveolin-1 and CD71 were used as resident protein markers of the lipid raft and non-lipid raft fractions, respectively. (B) The heparin–GPR56 interaction does not induce RhoA activation. Cell lysates of stable HT1080-GPR56 cells that had been stimulated with serum-free medium (lane 1), complete medium with 10% serum (lane 2) or heparin (20 µg/ml, lane 3) were subjected to the GTP-Rho pulldown assay, followed by western blot analysis using the mAb against RhoA, as described in the Materials and Methods. (C) The heparin–GPR56 interaction does not induce PKCα activation. Stable A375-GPR56 cells were treated without (lanes 1, 3) or with 20 µg/ml heparin (lanes 2, 4) for 30 min. Cells were lysed to collect lysates of the cytosolic fraction (Cyto) and membrane pellet fraction (MP). The cytosolic and membrane pellet fractions were probed with specific antibodies as indicated. The GPR56 NTF (detected with the CG4 mAb) and CD71 were used as resident protein markers of the cell membrane fraction. (D) Heparin binding to GPR56 interfered with the RhoA activation that was induced by the GPR56–collagen-III interaction. Left panel, representative western blot analysis of samples that had been subjected to the GTP-Rho pulldown assay using the mAb against RhoA. Samples include cell lysate of stable A375-Neo and A375-GPR56 cells with various treatments as indicated. # indicates cells were pre-incubated with the GPR56 binding partner first. Right panel, densitometry analysis of the active GTP-Rho protein bands. Values were normalized against the control total Rho protein bands detected in western blots (n=4, mean±s.e.m.; *P<0.05, **P<0.01, Student's t-test). (E–G) The heparin–GPR56 interaction reduces GPR56 receptor shedding. Levels of sGPR56 shed from transiently transfected GPR56-overexpressing HEK293T cells (E) and C32 melanoma cells (F), and from stable HT1080-GPR56 cells (G) after treatment with the indicated concentrations of heparin for 48 h. The levels of soluble GPR56 in conditioned medium were quantified using an ELISA-based assay, as described in the Materials and Methods. All data are means±s.e.m. of three independent experiments performed in triplicate. *P<0.05, **P<0.01, heparin-treated cells vs control cells (Student's t-test).

Journal of Cell Science (2016) 129, 2156-2169 doi:10.1242/jcs.174458

In fact, various adhesion GPCRs, such as CD97, EMR2 and GPR124, have been shown previously to interact with GAGs (Stacey et al., 2003; Vallon and Essler, 2006). Indeed, binding of chondroitin sulfate-B with CD97 and EMR2 is thought to play a role in the cellular interaction of activated T cells, dendritic cells and macrophages with B cells (Hamann et al., 1999; Stacey et al., 2003). The combinatorial interaction of CD97 with $\alpha_5\beta_1$ integrin and chondroitin sulfate synergistically enhances endothelial cell invasion (Wang et al., 2005), whereas the GAG-bound soluble GPR124 promotes endothelial cell survival by interacting with the $\alpha_v\beta_3$ integrin (Vallon and Essler, 2006). Hence, the interaction of GAGs and adhesion GPCRs is prevalent and functionally important.

The identification of the two major heparin-binding R^{26}GHREDFR^{33} and L^{190}KHPQKASRRP^{200} regions in GPR56 is consistent with the notion that clusters of basic residues, providing the electrostatic interaction, are important for heparin and heparan sulfate binding (Fig. 3). Interestingly, sequence comparison has shown that mouse GPR56 contains a similar basic residue composition (L^{190}QHPQKAAKRP^{200}) at the homologous region between positions 190 and 200, but lacks the reverse XBBXB consensus sequence (G^{26}SP**R**EDF**R**^{33}, basic residues in bold) as found in the most N-terminal sequence of human GPR56. This might explain the weaker heparin-binding activity of the mouse GPR56 protein. Because residual heparin-binding activity was still detected in the GPR56 probe where the seven basic residues [GPR56(1–340/7A)] had been mutated (Fig. 3D), the contribution to heparin binding of other basic residues in the NTF could not be completely ruled out.

It is known that residues proximal to the GAG-binding domains can influence the strength of GAG–protein interactions (Hileman et al., 1998; Lortat-Jacob et al., 2012). The stronger heparin-binding activity detected in BFPP-associated point mutants (R38W, Y88C and C91S) seems to reinforce this notion (Fig. 2). However, earlier molecular analyses have confirmed the tested BFPP point mutants are mostly intracellular misfolded proteins with a loss-of-function in collagen III binding (Luo et al., 2012). Hence, heparin-binding probably does not play a role in the development of BFPP. Rather, the stronger heparin-binding activity of these BFPP mutants is most likely due to conformational misfolding.

Heparin and heparan sulfate are known to greatly modulate the binding and function of many growth factors and cytokines to their cognate receptors (Pellegrini, 2001; Spivak-Kroizman et al., 1994; Yayon et al., 1991). As collagen III and TG2 themselves are also heparin-binding proteins (Lortat-Jacob et al., 2012; San Antonio et al., 1994), the overlapping and close proximity of the heparin-interacting domains with the collagen-III- and TG2-binding sites strongly suggest that heparin might modulate the interaction of GPR56 with its protein ligand(s) (Fig. S4). Indeed, this was subsequently confirmed by the differential effects of heparin on the ternary GPR56–heparin–protein-ligand interaction (Fig. 4A,B; Fig. S3F). It is not apparent why the GPR56–heparin interaction was inhibited by pre-incubation with collagen III and heparin, but not simultaneous addition of collagen III and heparin. However, it is interesting to note that although the heparin-binding and collagen-III-binding regions overlap, mutations of heparin-binding basic residues did not affect the collagen-III-binding activity of GPR56 (Fig. 3D). In sum, the differential ligand-binding effect is likely to be determined by multiple factors, such as the binding site occupancy, affinity and avidity of different individual GPR56–ligand interactions. Finally, the unexpected finding of the differential effects of GAGs on the interaction of GPR56 and the new cellular ligand further signifies that the new cellular protein ligand previously identified by us is distinct from collagen III (Fig. 4C,D). It will be of great interest to reveal its identity in the future.

The selective inhibition of the GPR56–heparin interaction by collagen III is more intriguing when the distinct effects of collagen III and heparin on GPR56 receptor shedding and GPR56-mediated cell migration are considered. As the ligand–receptor pair responsible for BFPP, the collagen-III–GPR56 interaction enhances GPR56 shedding, promotes the relocalization of the CTF to lipid raft microdomains and inhibits NPC migration by recruiting $G_{\alpha12}$ and $G_{\alpha13}$ proteins and promoting RhoA activation (Luo et al., 2011, 2014). Furthermore, mice deficient in *Col3a1* display neuronal over-migration and a cobblestone-like cortical malformation similar to that seen in BFPP.

By contrast, our results show that the heparin–GPR56 interaction reduces GPR56 shedding, and promotes cell adhesion and migration without apparent activation of known GPR56-mediated signaling molecules, such as RhoA and PKCα (Figs 5–7). The heparin–GPR56 interaction also does not promote CTF relocalization to lipid raft microdomains (Fig. 7A). As a highly expressed GAG molecule in the mammalian central nervous system (CNS), heparan sulfate is known to bind to a number of growth factors and morphogens, and to play a vital role in the embryonic brain development (Ford-Perriss et al., 2003; Inatani et al., 2003). Indeed, CNS-specific heparin-sulfate-deficient mice are known to display many developmental CNS defects owing to selective inhibition in midline axon guidance (Inatani et al., 2003). More recently, GPR56 has been found to be highly expressed in oligodendrocyte precursor cells (OPCs) and to act as an essential regulator of OPC proliferation and maturation to oligodendrocytes, which is important for CNS myelination (Ackerman et al., 2015; Giera et al., 2015). Interestingly, OPCs and oligodendrocytes express abundant levels of proteoglycans that are decorated by heparan sulfate (HSPGs) or chondroitin sulfate (CSPGs), some of which are known to be crucial in modulating OPC development and oligodendrocyte-mediated myelination positively or negatively (Harlow and Macklin, 2014; Kucharova and Stallcup, 2010; Pendleton et al., 2013; Properzi et al., 2008; Stringer et al., 1999; Szuchet et al., 2000). In summary, these findings are highly suggestive of a possible role of heparin and heparan sulfate in GPR56-regulated oligodendrocyte development.

Recent studies have revealed that shedding or removal of the NTF of adhesion GPCRs exposes a hidden Stächel sequence at the N-terminus of the CTF, which then acts as a tethered agonist for receptor activation (Liebscher et al., 2014; Stoveken et al., 2015). Our results show that heparin or heparan sulfate binding to GPR56 inhibits the dissociation of the GPR56 NTF from the CTF without inducing the known signaling activities (Fig. 7B–G). Most importantly, an inhibitory effect on collagen-III-induced RhoA activation was observed after heparin binding to GPR56 (Fig. 7D; Fig. S3G). This interesting feature is reminiscent of a receptor antagonist. Hence, it is possible that heparin and heparan sulfate act as a suppressor (antagonist) of GPR56 receptor function, in part, by inhibiting GPR56 receptor shedding, thereby trapping and masking the tethered Stächel peptide agonist and preventing the activation of the signaling pathways.

Outside the CNS, GPR56 also plays a pivotal role in many distinct biological systems, including male gonad development, myoblast fusion, muscle hypertrophy, hematopoietic stem cell generation and maintenance, tumor growth and metastasis, and cytotoxic immune cells. Heparin and heparan sulfate are present abundantly in many, if not all, of these cells, tissues and organs. Hence, the heparin–GPR56 interaction is expected to have more widespread functional

Journal of Cell Science (2016) 129, 2156-2169 doi:10.1242/jcs.174458

implications. Our results provide the first clue for a possible role of heparin in GPR56-mediated functions in these systems.

MATERIALS AND METHODS

General reagents and cell culture

Unless otherwise specified, general reagents were obtained from Sigma-Aldrich (Gillingham, Dorset, UK) or BDH-Merck (Poole, Dorset, UK). Oligonucleotide primers were supplied by Tri-I Biotech (Taipei, Taiwan). DNA and protein reagents were obtained from Invitrogen (Carlsbad, CA), Qiagen (Valencia, CA) and Amersham (GE Healthcare). The CG-2 and CG-3 monoclonal antibodies (mAb) against GPR56 have been described previously (5 µg/ml) (Yang et al., 2015). FITC-conjugated goat anti-mouse IgG was from Jackson ImmunoResearch (West Grove, PA). Mouse IgG_1 isotype control (clone 11711, 1:100) was from R&D Systems (Minneapolis, MN). Anti-TG2 mAb (clone CUB 7402, 1:200) was from Thermo Scientific (Fremont, CA). Anti-β-actin mAb (clone C4, 1:2000) was from Chemicon (Temecula, CA). Anti-7TM polyclonal antibodies were generated in rabbits immunized with the GPR56 cytoplasmic peptide NSDSARLPISSGSTSSSR. The anti-CD71 antibody (H68.4, 1:1000) was from Zymed Laboratories (San Francisco, CA), and the anti-caveolin-1 antibody (7C8, 1:1000) was from Upstate (Lake Placid, NY). Heparin (H4784) and GAGs (C3788, C4384, H7630 and H7640) were from Sigma-Aldrich. High-molecular-mass heparin (HEP001) and low-molecular-mass heparin (HO30) were from Amsbio (AMS Biotechnology, Oxon, UK). Human collagen III (ab73160) was from Abcam (Cambridge, UK). Human collagen IV (C5533) was from Sigma-Aldrich. Rat tail collagen I (354236) was from Becton Dickinson (Bedford, MA). Polyclonal PKCα antibody (C-20, 1:200) was from Santa Cruz Biotechnology, Inc. (Santa Cruz, CA). Heparin–agarose (H6508) and collagen–agarose beads (C0286) were from Sigma-Aldrich. All culture media were from Invitrogen (Carlsbad, CA) and were supplemented with 10% heat-inactivated FCS, 2 mM L-glutamine, 50 IU/ml penicillin and 50 µg/ml streptomycin. All cell lines used in this study were purchased from the American Type Culture Collection (Manassas, VA) and cultured in conditions as suggested. Briefly, HEK-293T and HT1080 cells were cultured in Dulbecco's Modified Eagle Medium (DMEM), whereas C32 melanoma and U87MG cells were cultured in minimum essential medium (MEM) containing non-essential amino acids and 1 mM sodium pyruvate.

Construction of expression vectors

The various truncated and mutated GPR56–mFc constructs were generated by PCR using GPR56–mFc cDNA as a template. The primer pairs used are listed in Table S1. The pFB-Neo retroviral construct encoding the full-length GPR56 receptor has been described previously (Hsiao et al., 2014). All expression constructs were sequenced to confirm their sequence fidelity.

Purification of mFc-fusion protein by protein-G affinity chromatography

The mFc-fusion proteins were purified from conditioned media using protein-G–Sepharose affinity chromatography as described previously (Chiang et al., 2011; Lin et al., 2005; Stacey et al., 2003). Briefly, conditioned media from transiently transfected HEK-293T cells were passed through the protein-G-conjugated Sepharose (nProtein-G Sepharose 4 Fast Flow, GE Healthcare), followed by extensive washes with washing buffer (50 mM Tris-HCl pH 7.4, 10 mM $CaCl_2$, 150 mM NaCl). The purified mFc-fusion proteins were stored at −80°C until use.

Retroviral infection and selection of stable HT1080 and A375 cell lines expressing GPR56

HEK-293T packaging cells in 10-cm dishes were transfected with 3 µg each of the pFB-Neo expression construct, pVPack-VSV-G and pVPack-GP vectors (Stratagene) with 25 µl of Lipofectamine in OPTI-MEM medium as recommended by the supplier. Virus-containing supernatant was harvested, and a final concentration of 5 µg/ml of polybrene solution was added. HT1080 and A375 cells (~40–50% confluence) in 6-well plates were infected with 1 ml of viral supernatant. The infected cells were selected in medium containing 1 mg/ml G418. G418-resistant cells were collected after ~2 weeks of selection and confirmed using appropriate analysis.

Solid-phase collagen-binding and GAG-binding assays

Protein–collagen-III binding was examined in 96-well tissue culture plates (Corning® 1×8 Stripwell™), whereas protein–GAG interactions were assessed in 96-well BD™ heparin-binding plates (BD Biosciences) coated with various GAGs. Briefly, collagens (5–30 µg/ml) and GAGs were dissolved in PBS and incubated in wells (100 µl/well) overnight at room temperature. The plate was washed extensively, then blocked with 0.2% gelatin blocking solution for 1 h at 37°C (for GAGs) or 1% BSA blocking solution for 1 h at room temperature (for collagens). Plates were incubated with the indicated protein probes for 2 h at room temperature. The plate was then washed extensively and incubated with mouse anti-human IL-8 mAb (1:250) (PeproTech, Rocky Hill, NJ) for the detection of IL-8, and/or with horseradish peroxidase (HRP)-conjugated goat anti-mouse Fc mAb (1:10,000) (Sigma-Aldrich) for the detection of mFc-fusion proteins in blocking buffer for 1 h at room temperature. The binding was revealed by incubation with tetramethylbenzidine substrate for 20 min and measured at OD_{450}.

Pulldown assay

Conditioned medium of HEK-293T cells that had been transiently transfected with the mFc-fusion-protein expression constructs was collected by centrifugation at 4°C for 10 min. Pulldown assays were performed using protein-G–agarose or heparin–agarose beads. Briefly, agarose beads (30 µl) were washed and then incubated with 500 µl blocking buffer (1% BSA in PBS) for 4 h at 4°C. Conditioned medium (3 ml) containing mFc-fusion protein was then incubated with the agarose beads at 4°C overnight with constant rotation. The beads were then washed extensively and boiled for 5 min in equal volumes of 2× SDS-PAGE sample buffer. The eluate was separated by SDS-PAGE and analyzed by western blotting.

Fluorescence-activated cell sorting cellular-ligand-binding assay

A modified cell-binding assay was performed essentially as described previously (Chiang et al., 2011). In brief, cells were subjected to the standard flow cytometry analysis using GPR56–mFc protein (10 µg/ml) as a probe. Cells were subsequently incubated with FITC-conjugated goat-anti mouse IgG (1:2000 in blocking buffer). Purified mFc protein (10 µg/ml) was used as a negative control. When necessary, protein ligands of GPR56, such as collagen III, were included as indicated. Binding was analyzed using a FACSCalibur Instrument (BD Bioscience). Data were analyzed by FlowJo 7.6.5 (Tree Star Inc., San Carlos, CA).

Cell adhesion assay

GAGs (10 µg/ml) were diluted in Hank's balanced salt solution (HBSS) and coated on 96-well BD™ heparin-binding plates (100 µl/well) overnight. The plate was washed with acetate buffer (100 mM NaCl, 50 mM NaOAc, 0.2% Tween-20, pH 7.2) before blocking with 0.2% gelatin blocking solution for 1 h at 37°C. A375 cells in suspension (1×10^6 cell/ml) were added to each well (100 µl/well) and incubated at 37°C for 30 min. After extensive washes, adherent cells were fixed with 100 µl of 1% glutaraldehyde (diluted in 0.1 M cacodylate buffer) per well for 30 min before staining with 100 µl of 1% Methylene Blue in 0.01 M borate buffer for 30 min. The excess dye was washed out, and 100 µl/well of ethanol was added. The dye dissolved in ethanol was transferred to another 96-well plate for measurement at OD_{595}.

Cell chemotaxis and invasion assays

Cell chemotaxis and invasion analyses were performed using a QCM Chemotaxis Cell Migration Assay kit and QCM ECMatrix Cell Invasion Assay Fluorimetric kit (Millipore, Bedford, MA), respectively, as described previously (Huang et al., 2012). In short, cells were serum-starved and resuspended at a density of 5×10^5 cells/ml in serum-free medium. Cells (100 µl/well) were placed in the upper chamber equipped with an 8-µm pore filter membrane. The bottom chambers were filled with medium with or without FCS (2% or 10%). The plates were kept in an incubator at 37°C for 6 h. Cells that had migrated were dissociated from the bottom of filter

membrane and stained with CyQuant GR dye. Fluorescence intensity was measured in a fluorescence plate reader (Molecular Devices) with a excitation 480-nm and emission 520-nm filter set.

GTP-Rho pulldown assay

The GTP-Rho pull-down assay was performed using A375-GPR56 stable cells. Cells at approximately 30% confluence were serum starved for 18 h, followed by the addition of heparin (20 µg/ml) for 30 min. Cells were then lysed in 150 µl of lysis buffer (50 mM Tris pH 7.5, 10 mM $MgCl_2$, 0.5 M NaCl and 2% Igepal). 400 µg of lysate proteins were incubated with 50 µg of beads conjugated with the GST-tagged Rho-binding domain of rhotekin (GST–RBD) (Cytoskeleton) at 4°C for 60 min. The beads were washed twice with wash buffer (25 mM Tris pH 7.5, 30 mM $MgCl_2$, 40 mM NaCl). Bound Rho proteins were eluted with Laemmli sample buffer and detected by western blotting using anti-RhoA mAb (Cytoskeleton, ARH03, 1:500).

Lipid raft separation

All procedures were performed on ice. Cells were washed, then lysed in 150 µl of ice-cold TNET buffer (25 mM Tris-HCl, pH 7.5, 150 mM NaCl, 5 mM EDTA, 1 mM EGTA, 1% Triton X-100, 10 mM NaF, 1 mM sodium pyrophosphate, 1 mM Na_3VO_4 and 1× protease inhibitor mixture) for 30 min. Total cell lysates were passed through a 25-gauge needle 20 times on ice, and then centrifuged at 1000 ***g*** for 10 min to collect the supernatant. Typically, 200 µl of cell lysate (~500 µg protein) were mixed with 400 µl of 60% OptiPrep™ gradient medium and then placed at the bottom of a 5 ml polyallomer ultracentrifuge tube (Beckman). Samples were overlaid sequentially with 3400 µl of 30% and 200 µl of 5% ice-cold OptiPrep™ gradient medium diluted in TNET buffer, and subjected to ultracentrifugation (Beckman) at 200,000 ***g*** for 16 h at 4°C. Following ultracentrifugation, seven equal fractions (~600 µl/fraction) were collected from the top of the tube for western blotting analyses.

Analysis of PKCα activation

For preparation of total cell membranes, cells were lysed in isotonic buffer without detergent (20 mM Tris–HCl, pH 7.5, 150 mM NaCl, 10 mM EDTA, 5 mM EGTA, 20 mM sodium fluoride, 5 mM sodium pyrophosphate, 1 mM sodium vanadate, 1 µM okadaic acid and a cocktail of protease inhibitors). Cell lysates were passed through a 25-gauge needle 20 times on ice and then centrifuged at 1000 ***g*** for 10 min at 4°C. The supernatant was further centrifuged at 300,000 ***g*** for 1 h at 4°C. The supernatant after the second centrifugation was designated as the cytosolic fraction, whereas the pellet encompassing total membrane proteins was analyzed by western blotting.

ELISA for the detection of soluble GPR56

sGPR56 was detected using a newly developed sandwich ELISA with minor modifications (Chen et al., 2011; Yang et al., 2015). Briefly, plates were coated with anti-GPR56 CG2 mAb (2 µg/ml) overnight at 4°C, followed by blocking for 1 h. Culture supernatant (100 µl/well) was added for 2-h incubations at 37°C. Following extensive washes, bound sGPR56 was detected using HRP-labeled CG3 mAb (5 µg/ml) and the peroxidase substrate. The absorbance was measured at 450 nm. All samples were analyzed in triplicate.

Statistics

Quantifications were based on at least three independent experiments. Data were shown as means±s.e.m. Statistical analysis of data was performed using the Student's *t*-test using Prism 5 software. *P*-values less than 0.05 were considered as significant.

Acknowledgements

We thank Dr Martin Stacey (University of Leeds, UK) for critical reading of the manuscript.

Competing interests

The authors declare no competing or financial interests.

Author contributions

H.H.L. designed and supervised the present study. N.-Y.C., G.-W.C., Y.-S.H., Y.-M.P., M.-L.K. and C.-C.H. performed the experiments. All authors contributed to the data analysis. N.-Y.C. and H.H.L. wrote the manuscript.

Funding

This study was supported in part by grants from the Ministry of Science and Technology, Taiwan [MOST101-2320-B-182-029-MY3 and MOST-104-2320-B-182-035-MY3 to H.-H.L., and MOST103-2811-B-182-002 to M.-L.K.]; and the Chang Gung Memorial Hospital, Linkou [grant numbers CMRPD1C0632-3, CMRPD1D0181-3 and CMRPD1D0391-3 to H.-H.L.].

Supplementary information

Supplementary information available online at
http://jcs.biologists.org/lookup/suppl/doi:10.1242/jcs.174458/-/DC1

References

Ackerman, S. D., Garcia, C., Piao, X., Gutmann, D. H. and Monk, K. R. (2015). The adhesion GPCR Gpr56 regulates oligodendrocyte development via interactions with Galpha12/13 and RhoA. *Nat. Commun.* **6**, 6122.

Araç, D., Boucard, A. A., Bolliger, M. F., Nguyen, J., Soltis, S. M., Südhof, T. C. and Brunger, A. T. (2012). A novel evolutionarily conserved domain of cell-adhesion GPCRs mediates autoproteolysis. *EMBO J.* **31**, 1364-1378.

Bernfield, M., Götte, M., Park, P. W., Reizes, O., Fitzgerald, M. L., Lincecum, J. and Zako, M. (1999). Functions of cell surface heparan sulfate proteoglycans. *Annu. Rev. Biochem.* **68**, 729-777.

Cardin, A. D. and Weintraub, H. J. (1989). Molecular modeling of protein-glycosaminoglycan interactions. *Arterioscler. Thromb. Vasc. Biol.* **9**, 21-32.

Carlsson, P., Presto, J., Spillmann, D., Lindahl, U. and Kjellen, L. (2008). Heparin/heparan sulfate biosynthesis: processive formation of N-sulfated domains. *J. Biol. Chem.* **283**, 20008-20014.

Chen, G., Yang, L., Begum, S. and Xu, L. (2010). GPR56 is essential for testis development and male fertility in mice. *Dev. Dyn.* **239**, 3358-3367.

Chen, T. Y., Hwang, T. L., Lin, C. Y., Lin, T. N., Lai, H. Y., Tsai, W. P. and Lin, H. H. (2011). EMR2 receptor ligation modulates cytokine secretion profiles and cell survival of lipopolysaccharide-treated neutrophils. *Chang Gung Med. J.* **34**, 468-477.

Chiang, N.-Y., Hsiao, C.-C., Huang, Y.-S., Chen, H.-Y., Hsieh, I.-J., Chang, G.-W. and Lin, H.-H. (2011). Disease-associated GPR56 mutations cause bilateral frontoparietal polymicrogyria via multiple mechanisms. *J. Biol. Chem.* **286**, 14215-14225.

Das, S., Owen, K. A., Ly, K. T., Park, D., Black, S. G., Wilson, J. M., Sifri, C. D., Ravichandran, K. S., Ernst, P. B. and Casanova, J. E. (2011). Brain angiogenesis inhibitor 1 (BAI1) is a pattern recognition receptor that mediates macrophage binding and engulfment of Gram-negative bacteria. *Proc. Natl. Acad. Sci. USA* **108**, 2136-2141.

Della Chiesa, M., Falco, M., Parolini, S., Bellora, F., Petretto, A., Romeo, E., Balsamo, M., Gambarotti, M., Scordamaglia, F., Tabellini, G. et al. (2010). GPR56 as a novel marker identifying the CD56dull CD16+ NK cell subset both in blood stream and in inflamed peripheral tissues. *Int. Immunol.* **22**, 91-100.

Drews, J. (2000). Drug discovery: a historical perspective. *Science* **287**, 1960-1964.

Esko, J. D., Kimata, K. and Lindahl, U. (2009). Chapter 16: proteoglycans and sulfated glycosaminoglycans. In *Essentials of Glycobiology* (ed. A. Varki, R. D. Cummings, J. D. Esko, H. H. Freeze, P. Stanley, C. R. Bertozzi, G. W. Hart and M. E. Etzler). New York: Cold Spring Harbor Laboratory Press.

Ford-Perriss, M., Turner, K., Guimond, S., Apedaile, A., Haubeck, H.-D., Turnbull, J. and Murphy, M. (2003). Localisation of specific heparan sulfate proteoglycans during the proliferative phase of brain development. *Dev. Dyn.* **227**, 170-184.

Funderburgh, J. L. (2000). Keratan sulfate: structure, biosynthesis, and function. *Glycobiology* **10**, 951-958.

Giera, S., Deng, Y., Luo, R., Ackerman, S. D., Mogha, A., Monk, K. R., Ying, Y., Jeong, S.-J., Makinodan, M., Bialas, A. R. et al. (2015). The adhesion G protein-coupled receptor GPR56 is a cell-autonomous regulator of oligodendrocyte development. *Nat. Commun.* **6**, 6121.

Hamann, J., Wishaupt, J. O., van Lier, R. A. W., Smeets, T. J. M., Breedveld, F. C. and Tak, P. P. (1999). Expression of the activation antigen CD97 and its ligand CD55 in rheumatoid synovial tissue. *Arthritis Rheum.* **42**, 650-658.

Hamann, J., Aust, G., Arac, D., Engel, F. B., Formstone, C., Fredriksson, R., Hall, R. A., Harty, B. L., Kirchhoff, C., Knapp, B. et al. (2015). International Union of Basic and Clinical Pharmacology. XCIV. Adhesion G protein-coupled receptors. *Pharmacol. Rev.* **67**, 338-367.

Harlow, D. E. and Macklin, W. B. (2014). Inhibitors of myelination: ECM changes, CSPGs and PTPs. *Exp. Neurol.* **251**, 39-46.

Hileman, R. E., Fromm, J. R., Weiler, J. M. and Linhardt, R. J. (1998). Glycosaminoglycan-protein interactions: definition of consensus sites in glycosaminoglycan binding proteins. *Bioessays* **20**, 156-167.

Hochreiter-Hufford, A. E., Lee, C. S., Kinchen, J. M., Sokolowski, J. D., Arandjelovic, S., Call, J. A., Klibanov, A. L., Yan, Z., Mandell, J. W. and Ravichandran, K. S. (2013). Phosphatidylserine receptor BAI1 and apoptotic cells as new promoters of myoblast fusion. *Nature* **497**, 263-267.

Hsiao, C.-C., Wang, W.-C., Kuo, W.-L., Chen, H.-Y., Chen, T.-C., Hamann, J. and Lin, H.-H. (2014). CD97 inhibits cell migration in human fibrosarcoma cells by modulating TIMP-2/MT1- MMP/MMP-2 activity–role of GPS autoproteolysis and functional cooperation between the N- and C-terminal fragments. *FEBS J.* **281**, 4878-4891.

Huang, Y.-S., Chiang, N.-Y., Hu, C.-H., Hsiao, C.-C., Cheng, K.-F., Tsai, W.-P., Yona, S., Stacey, M., Gordon, S., Chang, G.-W. et al. (2012). Activation of myeloid cell-specific adhesion class G protein-coupled receptor EMR2 via ligation-induced translocation and interaction of receptor subunits in lipid raft microdomains. *Mol. Cell. Biol.* **32**, 1408-1420.

Inatani, M., Irie, F., Plump, A. S., Tessier-Lavigne, M. and Yamaguchi, Y. (2003). Mammalian brain morphogenesis and midline axon guidance require heparan sulfate. *Science* **302**, 1044-1046.

Jeong, S.-J., Luo, R., Singer, K., Giera, S., Kreidberg, J., Kiyozumi, D., Shimono, C., Sekiguchi, K. and Piao, X. (2013). GPR56 functions together with alpha3beta1 integrin in regulating cerebral cortical development. *PLoS ONE* **8**, e68781.

Jin, Z., Tietjen, I., Bu, L., Liu-Yesucevitz, L., Gaur, S. K., Walsh, C. A. and Piao, X. (2007). Disease-associated mutations affect GPR56 protein trafficking and cell surface expression. *Hum. Mol. Genet.* **16**, 1972-1985.

Kaur, B., Brat, D. J., Devi, N. S. and Van Meir, E. G. (2005). Vasculostatin, a proteolytic fragment of brain angiogenesis inhibitor 1, is an antiangiogenic and antitumorigenic factor. *Oncogene* **24**, 3632-3642.

Krasnoperov, V., Lu, Y., Buryanovsky, L., Neubert, T. A., Ichtchenko, K. and Petrenko, A. G. (2002). Post-translational proteolytic processing of the calcium-independent receptor of alpha-latrotoxin (CIRL), a natural chimera of the cell adhesion protein and the G protein-coupled receptor. Role of the G protein-coupled receptor proteolysis site (GPS) motif. *J. Biol. Chem.* **277**, 46518-46526.

Kucharova, K. and Stallcup, W. B. (2010). The NG2 proteoglycan promotes oligodendrocyte progenitor proliferation and developmental myelination. *Neuroscience* **166**, 185-194.

Liebscher, I., Schön, J., Petersen, S. C., Fischer, L., Auerbach, N., Demberg, L. M., Mogha, A., Cöster, M., Simon, K.-U., Rothemund, S. et al. (2014). A tethered agonist within the ectodomain activates the adhesion G protein-coupled receptors GPR126 and GPR133. *Cell Rep.* **9**, 2018-2026.

Liebscher, I., Monk, K. R. and Schöneberg, T. (2015). How to wake a giant. *Oncotarget* **6**, 23038-23039.

Lin, H.-H., Chang, G.-W., Davies, J. Q., Stacey, M., Harris, J. and Gordon, S. (2004). Autocatalytic cleavage of the EMR2 receptor occurs at a conserved G protein-coupled receptor proteolytic site motif. *J. Biol. Chem.* **279**, 31823-31832.

Lin, H.-H., Stacey, M., Chang, G.-W., Davies, J. Q. and Gordon, S. (2005). Method for selecting and enriching cells expressing low affinity ligands for cell surface receptors. *Biotechniques* **38**, 696-698.

Little, K. D., Hemler, M. E. and Stipp, C. S. (2004). Dynamic regulation of a GPCR-tetraspanin-G protein complex on intact cells: central role of CD81 in facilitating GPR56-Galpha q/11 association. *Mol. Biol. Cell* **15**, 2375-2387.

Liu, M., Parker, R. M. C., Darby, K., Eyre, H. J., Copeland, N. G., Crawford, J., Gilbert, D. J., Sutherland, G. R., Jenkins, N. A. and Herzog, H. (1999). GPR56, a novel secretin-like human G-protein-coupled receptor gene. *Genomics* **55**, 296-305.

Lortat-Jacob, H., Burhan, I., Scarpellini, A., Thomas, A., Imberty, A., Vives, R. R., Johnson, T., Gutierrez, A. and Verderio, E. A. M. (2012). Transglutaminase-2 interaction with heparin: identification of a heparin binding site that regulates cell adhesion to fibronectin-transglutaminase-2 matrix. *J. Biol. Chem.* **287**, 18005-18017.

Luo, R., Jeong, S.-J., Jin, Z., Strokes, N., Li, S. and Piao, X. (2011). G protein-coupled receptor 56 and collagen III, a receptor-ligand pair, regulates cortical development and lamination. *Proc. Natl. Acad. Sci. USA* **108**, 12925-12930.

Luo, R., Jin, Z., Deng, Y., Strokes, N. and Piao, X. (2012). Disease-associated mutations prevent GPR56-collagen III interaction. *PLoS ONE* **7**, e29818.

Luo, R., Jeong, S.-J., Yang, A., Wen, M., Saslowsky, D. E., Lencer, W. I., Araç, D. and Piao, X. (2014). Mechanism for adhesion G Protein-Coupled Receptor GPR56-mediated RhoA activation induced by collagen III stimulation. *PLoS ONE* **9**, e100043.

Ma, P. and Zemmel, R. (2002). Value of novelty? *Nat. Rev. Drug Discov.* **1**, 571-572.

Paavola, K. J., Stephenson, J. R., Ritter, S. L., Alter, S. P. and Hall, R. A. (2011). The N terminus of the adhesion G protein-coupled receptor GPR56 controls receptor signaling activity. *J. Biol. Chem.* **286**, 28914-28921.

Pellegrini, L. (2001). Role of heparan sulfate in fibroblast growth factor signalling: a structural view. *Curr. Opin. Struct. Biol.* **11**, 629-634.

Pendleton, J. C., Shamblott, M. J., Gary, D. S., Belegu, V., Hurtado, A., Malone, M. L. and McDonald, J. W. (2013). Chondroitin sulfate proteoglycans inhibit oligodendrocyte myelination through PTPsigma. *Exp. Neurol.* **247**, 113-121.

Peng, Y.-M., van de Garde, M. D. B., Cheng, K.-F., Baars, P. A., Remmerswaal, E. B. M., van Lier, R. A. W., Mackay, C. R., Lin, H.-H. and Hamann, J. (2011). Specific expression of GPR56 by human cytotoxic lymphocytes. *J. Leukoc. Biol.* **90**, 735-740.

Piao, X., Hill, R. S., Bodell, A., Chang, B. S., Basel-Vanagaite, L., Straussberg, R., Dobyns, W. B., Qasrawi, B., Winter, R. M., Innes, A. M. et al. (2004). G protein-coupled receptor-dependent development of human frontal cortex. *Science* **303**, 2033-2036.

Properzi, F., Lin, R., Kwok, J., Naidu, M., van Kuppevelt, T. H., ten Dam, G. B., Camargo, L. M., Raha-Chowdhury, R., Furukawa, Y., Mikami, T. et al. (2008). Heparan sulphate proteoglycans in glia and in the normal and injured CNS: expression of sulphotransferases and changes in sulphation. *Eur. J. Neurosci.* **27**, 593-604.

Rabenstein, D. L. (2002). Heparin and heparan sulfate: structure and function. *Nat. Prod. Rep.* **19**, 312-331.

Saito, Y., Kaneda, K., Suekane, A., Ichihara, E., Nakahata, S., Yamakawa, N., Nagai, K., Mizuno, N., Kogawa, K., Miura, I. et al. (2013). Maintenance of the hematopoietic stem cell pool in bone marrow niches by EVI1-regulated GPR56. *Leukemia* **27**, 1637-1649.

Salmivirta, M., Lidholt, K. and Lindahl, U. (1996). Heparan sulfate: a piece of information. *FASEB J.* **10**, 1270-1279.

San Antonio, J. D., Karnovsky, M. J., Gay, S., Sanderson, R. D. and Lander, A. D. (1994). Interactions of syndecan-1 and heparin with human collagens. *Glycobiology* **4**, 327-332.

Schoneberg, T., Liebscher, I., Luo, R., Monk, K. R. and Piao, X. (2015). Tethered agonists: a new mechanism underlying adhesion G protein-coupled receptor activation. *J. Recept. Signal. Transduct. Res.* **35**, 220-223.

Solaimani Kartalaei, P., Yamada-Inagawa, T., Vink, C. S., de Pater, E., van der Linden, R., Marks-Bluth, J., van der Sloot, A., van den Hout, M., Yokomizo, T., van Schaick-Solerno, M. L. et al. (2015). Whole-transcriptome analysis of endothelial to hematopoietic stem cell transition reveals a requirement for Gpr56 in HSC generation. *J. Exp. Med.* **212**, 93-106.

Spivak-Kroizman, T., Lemmon, M. A., Dikic, I., Ladbury, J. E., Pinchasi, D., Huang, J., Jaye, M., Crumley, G., Schlessinger, J. and Lax, I. (1994). Heparin-induced oligomerization of FGF molecules is responsible for FGF receptor dimerization, activation, and cell proliferation. *Cell* **79**, 1015-1024.

Stacey, M., Lin, H.-H., Gordon, S. and McKnight, A. J. (2000). LNB-TM7, a group of seven-transmembrane proteins related to family-B G-protein-coupled receptors. *Trends Biochem. Sci.* **25**, 284-289.

Stacey, M., Chang, G.-W., Davies, J. Q., Kwakkenbos, M. J., Sanderson, R. D., Hamann, J., Gordon, S. and Lin, H.-H. (2003). The epidermal growth factor-like domains of the human EMR2 receptor mediate cell attachment through chondroitin sulfate glycosaminoglycans. *Blood* **102**, 2916-2924.

Stoveken, H. M., Hajduczok, A. G., Xu, L. and Tall, G. G. (2015). Adhesion G protein-coupled receptors are activated by exposure of a cryptic tethered agonist. *Proc. Natl. Acad. Sci. USA* **112**, 6194-6199.

Stringer, S. E., Mayer-Proschel, M., Kalyani, A., Rao, M. and Gallagher, J. T. (1999). Heparin is a unique marker of progenitors in the glial cell lineage. *J. Biol. Chem.* **274**, 25455-25460.

Szuchet, S., Watanabe, K. and Yamaguchi, Y. (2000). Differentiation/regeneration of oligodendrocytes entails the assembly of a cell-associated matrix. *Int. J. Dev. Neurosci.* **18**, 705-720.

Trowbridge, J. M. and Gallo, R. L. (2002). Dermatan sulfate: new functions from an old glycosaminoglycan. *Glycobiology* **12**, 117R-125R.

Vallon, M. and Essler, M. (2006). Proteolytically processed soluble tumor endothelial marker (TEM) 5 mediates endothelial cell survival during angiogenesis by linking integrin alpha(v)beta3 to glycosaminoglycans. *J. Biol. Chem.* **281**, 34179-34188.

Wang, T., Ward, Y., Tian, L., Lake, R., Guedez, L., Stetler-Stevenson, W. G. and Kelly, K. (2005). CD97, an adhesion receptor on inflammatory cells, stimulates angiogenesis through binding integrin counterreceptors on endothelial cells. *Blood* **105**, 2836-2844.

White, J. P., Wrann, C. D., Rao, R. R., Nair, S. K., Jedrychowski, M. P., You, J.-S., Martinez-Redondo, V., Gygi, S. P., Ruas, J. L., Hornberger, T. A. et al. (2014). G protein-coupled receptor 56 regulates mechanical overload-induced muscle hypertrophy. *Proc. Natl. Acad. Sci. USA* **111**, 15756-15761.

Wu, M. P., Doyle, J. R., Barry, B., Beauvais, A., Rozkalne, A., Piao, X., Lawlor, M. W., Kopin, A. S., Walsh, C. A. and Gussoni, E. (2013). G-protein coupled receptor 56 promotes myoblast fusion through serum response factor- and nuclear factor of activated T-cell-mediated signalling but is not essential for muscle development in vivo. *FEBS J.* **280**, 6097-6113.

Xu, L., Begum, S., Hearn, J. D. and Hynes, R. O. (2006). GPR56, an atypical G protein-coupled receptor, binds tissue transglutaminase, TG2, and inhibits melanoma tumor growth and metastasis. *Proc. Natl. Acad. Sci. USA* **103**, 9023-9028.

Yang, L., Chen, G., Mohanty, S., Scott, G., Fazal, F., Rahman, A., Begum, S., Hynes, R. O. and Xu, L. (2011). GPR56 regulates VEGF production and angiogenesis during melanoma progression. *Cancer Res.* **71**, 5558-5568.

Yang, L., Friedland, S., Corson, N. and Xu, L. (2014). GPR56 inhibits melanoma growth by internalizing and degrading its ligand TG2. *Cancer Res.* **74**, 1022-1031.

Yang, T.-Y., Chiang, N.-Y., Tseng, W.-Y., Pan, H.-L., Peng, Y.-M., Shen, J.-J., Wu, K.-A., Kuo, M.-L., Chang, G.-W. and Lin, H.-H. (2015). Expression and

Journal of Cell Science

Journal of Cell Science (2016) 129, 2156-2169 doi:10.1242/jcs.174458

immunoaffinity purification of recombinant soluble human GPR56 protein for the analysis of GPR56 receptor shedding by ELISA. *Protein Expr. Purif.* **109**, 85-92.

Yayon, A., Klagsbrun, M., Esko, J. D., Leder, P. and Ornitz, D. M. (1991). Cell surface, heparin-like molecules are required for binding of basic fibroblast growth factor to its high affinity receptor. *Cell* **64**, 841-848.

Yona, S., Lin, H.-H., Siu, W. O., Gordon, S. and Stacey, M. (2008). Adhesion-GPCRs: emerging roles for novel receptors. *Trends Biochem. Sci.* **33**, 491-500.

Zendman, A. J. W., Cornelissen, I. M. H. A., Weidle, U. H., Ruiter, D. J. and van Muijen, G. N. P. (1999). TM7XN1, a novel human EGF-TM7-like cDNA, detected with mRNA differential display using human melanoma cell lines with different metastatic potential. *FEBS Lett.* **446**, 292-298.